Parity Doubling and the S Parameter Below the Conformal Window

T. Appelquist,[1] R. Babich,[2] R. C. Brower,[2] M. Cheng,[3] M. A. Clark,[4] S. D. Cohen,[2] G. T. Fleming,[1] J. Kiskis,[5] M. F. Lin,[1] E. T. Neil,[1] J. C. Osborn,[6] C. Rebbi,[2] D. Schaich,[2] and P. Vranas[3]

(Lattice Strong Dynamics (LSD) Collaboration)

[1]*Department of Physics, Sloane Laboratory, Yale University, New Haven, Connecticut 06520, USA*
[2]*Department of Physics, Boston University, Boston, Massachusetts 02215, USA*
[3]*Physical Sciences Directorate, Lawrence Livermore National Laboratory, Livermore, California 94550, USA*
[4]*Harvard-Smithsonian Center for Astrophysics, Cambridge, Massachusetts 02138, USA*
[5]*Department of Physics, University of California, Davis, California 95616, USA*
[6]*Argonne Leadership Computing Facility, Argonne, Illinois 60439, USA*

We describe a lattice simulation of the masses and decay constants of the lowest-lying vector and axial resonances, and the electroweak S parameter, in an $SU(3)$ gauge theory with $N_f = 2$ and 6 fermions in the fundamental representation. The spectrum becomes more parity doubled and the S parameter per electroweak doublet decreases when N_f is increased from 2 to 6, motivating study of these trends as N_f is increased further, toward the critical value for transition from confinement to infrared conformality.

PACS numbers: 11.10.Hi, 11.15.Ha, 11.25.Hf, 12.60.Nz

Introduction In a recent letter [1], we studied the chiral properties of an SU(3) gauge theory with N_f massless Dirac fermions in the fundamental representation as N_f is increased from 2 to 6. We noted that the $N_f = 2$ simulations are in good agreement with measured QCD values, and that the $N_f = 6$ results indicate substantial enhancement of the chiral condensate. Here we extend our study of these two theories, presenting results for the electroweak S parameter and for the lightest vector and axial resonances.

For an SU(N) gauge theory, lattice simulations [2–6] suggest infrared conformality exists for N_f values from the onset of asymptotic freedom down to a critical value N_f^c. A fixed point (whose value depends on the defining scheme) governs the infrared behavior. Below this "conformal window", chiral symmetry breaking and confinement set in. Even for $N_f < N_f^c$ studies using continuum gap equations suggest that there can remain an approximate infrared fixed point provided that $0 < N_f^c - N_f \ll N_f^c$. The scale of chiral symmetry breaking is small compared to some high scale where asymptotic freedom sets in, and the fixed point approximately governs the theory from the breaking scale to this higher scale. This "walking" behavior leads to chiral-condensate enhancement, which can address the problem of obtaining large enough quark and lepton masses in technicolor theories.

It has been suggested [7–9] that walking theories could address another problem by leading to smaller values of the electroweak S parameter. The value of S is related to the spectrum of vector and axial resonances in the theory. As in Ref. [1], we start with $N_f = 2$, allowing us to check the reliability of our methods by comparison with QCD phenomenology. We then consider the $N_f = 6$ theory in which the coupling runs more slowly than in the $N_f = 2$ theory, but which is not yet truly walking. Proceeding carefully toward N_f^c is prudent since the eventual appearance of widely separated scales associated with walking is challenging for lattice methods.

We first compute the S parameter from the defining current correlators, and then present results for the lowest lying vector and axial masses and decay constants. We discuss our results along with the related Weinberg spectral function sum rules, and then summarize.

The S parameter The S parameter can be defined in terms of the vector and axial current-correlation functions with, by convention, the would-be Nambu-Goldstone-boson (NGB) contribution to the standard-model (SM) radiative corrections removed. With $N_f/2$ massless electroweak doublets, it can be written as [10]

$$\begin{aligned} S &= 4\pi(N_f/2)\left[\Pi'_{VV}(0) - \Pi'_{AA}(0)\right] - \Delta S_{SM} \\ &= \frac{1}{3\pi}\int_0^\infty \frac{ds}{s}\left\{(N_f/2)\left[R_V(s) - R_A(s)\right]\right. \\ &\qquad \left. -\frac{1}{4}\left[1 - \left(1 - \frac{m_H^2}{s}\right)^3 \theta(s - m_H^2)\right]\right\}, \end{aligned} \tag{1}$$

where $\Pi_{VV}(Q^2)$ and $\Pi_{AA}(Q^2)$ are the transverse correlation functions for a single electroweak doublet, $R(s) \equiv 12\pi \,\mathrm{Im}\,\Pi'(s)$, and m_H is the reference Higgs mass. The presence of $R_V(s) - R_A(s)$ in the spectral integral suggests that S could decrease if the resonance spectrum becomes more parity doubled with increasing N_f.

For $N_f = 2$, there are 3 Goldstone bosons, with the $I_3 = 1$ pair leading to $R_V(s) \to 1/4$ as $s \to 0$. ($R_A(s) \to 0$.) The standard-model subtraction removes the resultant infrared divergence. With $N_f/2$ electroweak doublets, there are $N_f^2 - 1$ NGB's in the absence of other interactions. Among these, $(N_f/2)^2$ pairs contribute to S, leading to $R_V(0) = (1/4)N_f/2$. With standard-model and other interactions included, $N_f^2 - 4$ of the $N_f^2 - 1$ Goldstone bosons will be pseudo-Nambu-Goldstone bosons (PNGBs). The S parameter is again infrared finite, depending logarithmically on the masses of the PNGBs.

Lattice simulations are carried out with a finite fermion mass m_f, requiring extrapolation to reach the chiral limit. With $N_f/2$ electroweak doublets, since we do not include SM and other interactions to give mass to the PNGBs, the extrapolation for $N_f \neq 2$ would lead to log m_f terms in S. For our simulations, m_f is not yet small enough to see clear evidence for these chiral logs.

Simulation Details Simulations are performed using domain-wall fermions and the Iwasaki improved gauge action [11]. The domain-wall formulation suppresses the chiral symmetry breaking associated with fermion discretization, and preserves flavor symmetry at finite lattice spacing, both desirable properties for computation of the S-parameter. Gauge configurations are generated as in Ref. [1]. Dimensionful quantities are given in lattice units. The lattice volume is set to $32^3 \times 64$, with the length of the fifth dimension $L_s = 16$ and the domain-wall height $m_0 = 1.8$. With the choices $\beta = 2.70$ for $N_f = 2$ and $\beta = 2.10$ for $N_f = 6$, the physical scales represented by the mass of the lightest vector resonance, are the same within errors. For the NGB decay constants, the chiral extrapolation for $N_f = 6$ is not yet possible, so it remains open whether they are the same in the chiral limit [1].

Simulations are performed for fermion masses $m_f = 0.005$ to 0.03, although the $N_f = 2$ results for $m_f = 0.005$ may suffer from finite-volume effects, and are not included in the analysis. For other values of m_f, $M_P L > 4$, so that finite-volume effects should be small. Other systematic effects, for example due to the finite lattice spacing are also believed to be small. The error bars shown in each figure are therefore statistical. At finite lattice spacing, even with $m_f = 0$, the chiral symmetry is not exact, with the violation captured in a small residual mass m_{res} ($= 2.63(2) \times 10^{-5}$ for $N_f = 2$ and $8.26(3) \times 10^{-4}$ for $N_f = 6$). The total fermion mass m is then $m \equiv m_f + m_{res}$.

Current Correlators The lattice expression for the current correlator of interest is

$$\begin{aligned} \Pi^{\mu\nu}_{VV}(Q) &= \delta^{\mu\nu}\Pi_{VV}(Q^2) - (Q^\mu Q^\nu/Q^2)\widetilde{\Pi}_{VV}(Q^2) \\ &= Z\sum_x e^{iQ\cdot(x+\hat{\mu}/2)}\langle \mathcal{V}^\mu(x) V^\nu(0)\rangle \end{aligned} \qquad (2)$$

and similarly for Π_{AA}. Here $\mathcal{V}^\mu$ is the conserved domain-wall vector current, V^ν is the non-conserved local current, and Z is a non-perturbative renormalization constant. $(x + \hat{\mu}/2)$ appears because $\mathcal{V}^\mu(x)$ is point split on the link $(x, x + \mu)$. The use of conserved currents ensures that lattice artifacts cancel in the $V - A$ current correlator $\Pi_{V-A}(Q^2) \equiv \Pi_{VV}(Q^2) - \Pi_{AA}(Q^2)$ [12].

We calculate $\Pi_{V-A}(Q^2)$ for a range of positive (spacelike) Q^2 values, and for each m_f extrapolate to $Q^2 = 0$ to determine the slope $4\pi\Pi'_{V-A}(0)$ entering the S parameter. In Fig. 1, we show the simulation data for $\Pi_{V-A}(Q^2)$, along with statistical errors and fit curves. The data itself

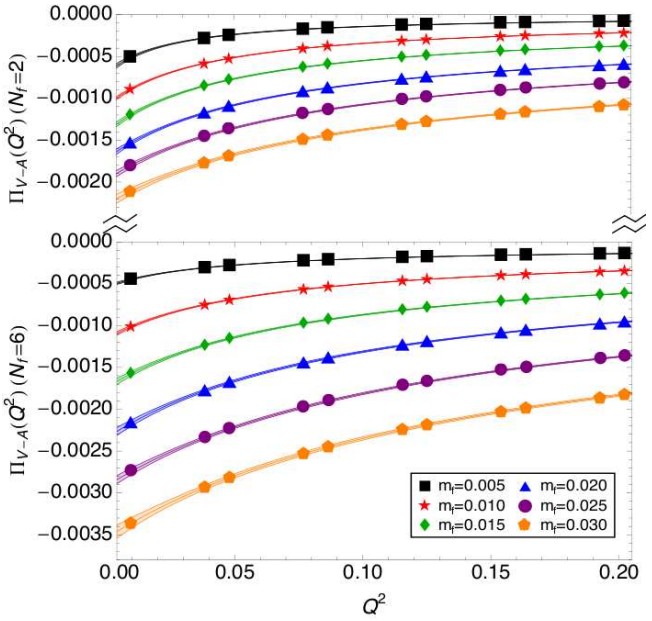

FIG. 1: $\Pi_{V-A}(Q^2)$ data and fits for $N_f = 2$ and 6. Fits, over the range $Q^2 < 0.40$, are done separately for each m_f.

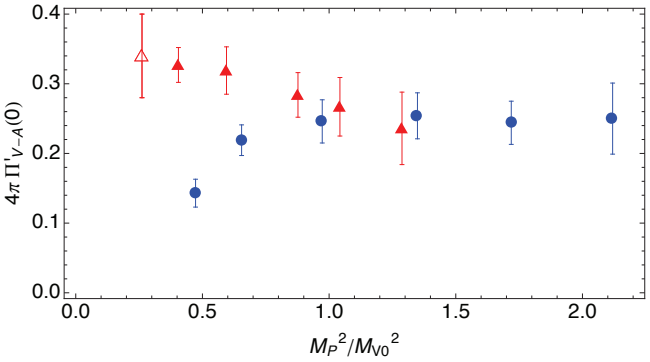

FIG. 2: $V - A$ correlator slopes at $Q^2 = 0$ for $N_f = 2$ (red triangles) and $N_f = 6$ (blue circles). For each of the solid points, $M_P L > 4$.

indicates that for $N_f = 2$, $\Pi'_{V-A}(0)$ increases as m_f decreases, while for $N_f = 6$, it decreases, suggesting a relative decrease in S per electroweak doublet at $N_f = 6$. We fit the $\Pi_{V-A}(Q^2)$ data for $Q^2 < 0.4$ using a four-parameter, Pade(1,2) form (linear numerator, quadratic denominator). These fits, behaving like $1/Q^2$ at large positive Q^2, are shown with statistical error bands in Fig. 1. Each has two poles at real, negative Q^2, representing a time-like structure with cuts and multiple poles. Each fit leads to a value of $\Pi'_{V-A}(0)$ stable as the number of Q^2 points is varied.

The correlator slopes at $Q^2 = 0$ are plotted in Fig. 2. In this figure and others, we plot versus M_P^2/M_{V0}^2 rather than m, where M_P is the NGB mass [1], and M_{V0} is the extrapolated mass of the lightest vector state. M_P^2/M_{V0}^2 is more directly physical, and the relation between M_P^2 and

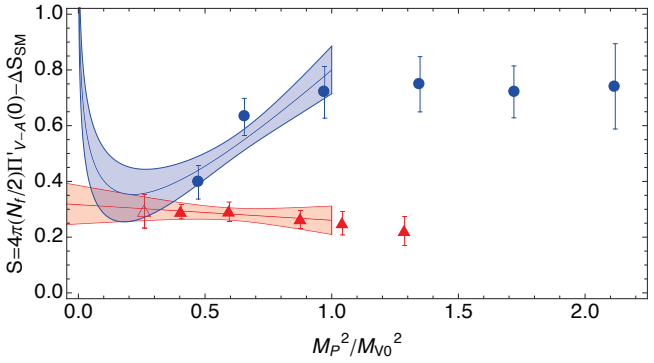

FIG. 3: S parameter for $N_f = 2$ (red triangles) and $N_f = 6$ (blue circles). For each of the solid points, $M_P L > 4$. The bands correspond to fits explained in the text.

m is strongly N_f-dependent. The value of M_{V0}, to be discussed later, is roughly 0.2 in lattice units for both $N_f = 2$ and 6. For each of the solid points, $M_P L > 4$. As anticipated from the data in Fig. 1, $\Pi'_{V-A}(0)$ at $N_f = 6$ drops below $\Pi'_{V-A}(0)$ at $N_f = 2$ for the smaller M_P^2 values, suggesting a suppression of S at $N_f = 6$. This interpretation requires care, however, since the extrapolation $M_P^2 \propto m \to 0$ is dominated by chiral logs for both $N_f = 2$ and 6.

S-Parameter Results The S parameter (Eq. 1) is simply the correlator slope multiplied by the number of electroweak doublets, with the SM subtraction. We estimate the SM subtraction by evaluating the ΔS_{SM} integral in Eq. 1 with an infrared cutoff at $s = 4M_P^2$, and taking $m_H = M_{V0}$. For the case $2M_P < M_{V0}$,

$$\Delta S_{SM}(M_P) = \frac{1}{12\pi}\left[\frac{11}{6} + \log\left(\frac{M_{V0}^2}{4M_P^2}\right)\right]. \quad (3)$$

We use values for M_P and M_{V0} determined in Ref. [1]. The choice $m_H = M_{V0}$ corresponds roughly to a 1 TeV value for the reference Higgs mass.

In Fig. 3, we plot $S \equiv 4\pi(N_f/2)\Pi'_{V-A}(0) - \Delta S_{SM}$. For $N_f = 2$, the results are consistent with previous lattice simulations [12, 13]. The SM subtraction at $N_f = 2$ is small, reaching a value ~ 0.04 for the lowest solid mass point, corresponding to $m_f = 0.010$. A smooth extrapolation to $M_P^2 = 0$ is expected since the LO chiral logs eventually appearing in $\Pi'_{V-A}(0)$ are canceled by the SM subtraction, Eq. 3. Given the linearity of the solid data points, we include a linear fit to the three solid points with $M_P^2/M_{V0}^2 < 1$. In this range, where chiral perturbation theory should begin to be applicable, there can also be an NLO term of the form $M_P^2 \log M_P^2$, but it is not visible in our data so we disregard it. The fit, with error band, is shown in Fig. 3, giving $S_{m=0} = 0.32(5)$, consistent with the value obtained using scaled-up QCD data [10].

The $N_f = 6$ results for S are also shown in Fig. 3. The SM subtraction is again very small. For the higher mass points, S is consistent with a value obtained by simply scaling up the $N_f = 2$ points by a factor of 3. The value of S at the lower mass points, where $M_P^2/M_{V0}^2 < 1$, begins to drop well below its value at the higher mass points. This trend has appeared at $N_f = 6$ even though $6 \ll N_f^c$. As M_P^2 is decreased further at $N_f = 6$, S as computed here will eventually turn up since the SM subtraction leaves the chiral-log contribution $(1/12\pi)[N_f^2/4 - 1] \log M_P^{-2}$. To estimate where this turn-up sets in, we include a simple fit of the form $S = A + BM_P^2 + (2/3\pi)\log(M_{V0}^2/M_P^2)$ to the three points with $M_P^2/M_{V0}^2 < 1$, disregarding a possible $M_P^2 \log M_P^2$ term. This fit, with error band, is also shown in Fig. 3. In a realistic context, of course, the PNGBs receive mass even in the limit $m \to 0$ from SM and other interactions not included here, and these masses provide the infrared cutoff in the logs.

Resonance Spectrum A question of general interest for an $SU(N)$ gauge theory is the form of the resonance spectrum as N_f is increased toward N_f^c. A trend toward parity doubling, for example, would provide a striking contrast with a QCD-like theory. If the gauge theory plays a role in electroweak symmetry breaking, then this trend could be associated with a diminished S parameter.

We have so far computed the masses, M_V and M_A, and decay constants, F_V and F_A, of the lowest-lying vector and axial resonances. We plot the masses along with their ratio in Fig. 4. Since the solid data points ($M_P L > 4$) are quite linear with a small slope for each case except M_A at $N_f = 6$, and since in each case, the NLO term in chiral perturbation theory is linear in $M_P^2 \propto m$, we include a linear fit to *all* the solid points. The error bars on the extrapolations are also shown. For $N_f = 2$, M_V extrapolates to $0.215(3)$ and for $N_f = 6$ it extrapolates to $0.209(3)$. As noted above, the equality within errors of these two masses in lattice units was arranged by the choice of the lattice coupling in each case.

For $N_f = 2$, the extrapolated value of $M_A/M_V = 1.476(40)$ is roughly consistent with the experimental result of 1.585(52) [14]. The $N_f = 6$ data points for M_A do not yet allow a simple fit and extrapolation, However, they do indicate a substantial decrease in M_A/M_V for $M_P^2/M_{V0}^2 < 1$, the same range for which the S parameter begins to drop for $N_f = 6$, indicating that the decrease in S is indeed associated with a trend toward parity doubling.

Our simulation results for F_V and F_A, using the normalization conventions of Ref. [10], will be presented in a future paper. The dependence on M_P^2/M_{V0}^2 is mild, and for each case except the F_A at $N_f = 6$, quite linear with a small slope. Although there is known to be an NLO chiral log for the decay constants, it is not visible in these cases, so we have performed a linear fit to the data. We simply report here that for $N_f = 2$ the linearly extrapolated values, converted to physical units using the lattice scale determined from M_{V0}, are $F_V = 141.8(3.8)$ MeV and $F_A = 138.9(8.2)$ MeV, agreeing well with the measured QCD results [11, 15].

Discussion The relation between a diminished S parameter and the spectrum can be explored through the dis-

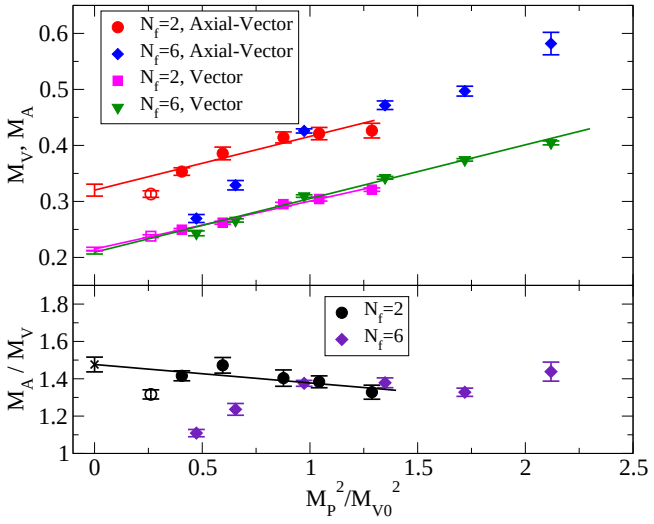

FIG. 4: Axial and vector masses, M_A and M_V, and their ratio. Straight lines show linear fits to the solid points ($M_P L > 4$), with the extrapolated values and errors shown to the left.

persion relation

$$\Pi_{V-A}(Q^2) = \frac{Q^2}{12\pi}\int_0^\infty \frac{ds}{\pi}\frac{R_V(s)-R_A(s)}{s+Q^2} - F_P^2\,, \quad (4)$$

where $F_P \simeq 93$ MeV for two-flavor QCD. Here, we include a few remarks about this use of the dispersion relation via the assumption of single-pole dominance.

As a preliminary, recall that in the chiral limit (and in the continuum), the operator product expansion gives $\Pi_{V-A}(Q^2) \sim 1/Q^4$ as $Q^2 \to \infty$. In the resultant first and second (integral) Weinberg sum rules (WSRs), the assumption of single pole dominance, $R_{V,A}(s) = 12\pi^2 F_{V,A}^2 \delta(s - M_{V,A}^2)$, then leads to the relations $F_V^2 - F_A^2 = F_P^2$ and $F_V^2 M_V^2 - F_A^2 M_A^2 = 0$. At finite m, however, $\Pi_{V-A}(Q^2)$ falls more slowly with Q^2. The simulation data in the Q^2 range of Fig. 1 behaves like $m\langle\bar\psi\psi\rangle/Q^2$, but there will be an additional small ($O(m^2)$) term [16]. While the data are consistent with the first WSR, the single-pole-dominance relation $F_V^2 - F_A^2 = F_P^2$ is not satisfied at $N_f = 2$ for any m, the LHS being less than 50% of the RHS. The extrapolated values and the QCD experimental values fail by even more. A similar discussion applies to the second WSR at $N_f = 2$ and the resultant pole-dominance relation. For $N_f = 6$, the errors on F_A do not yet allow a useful test.

Turning to the S parameter, a crude expression deriving from the $Q^2 \to 0$ limit of the dispersion relation can be obtained by assuming single-pole dominance, and neglecting the SM subtraction. The result, $S = 4\pi(N_f/2)[F_V^2/M_V^2 - F_A^2/M_A^2]$, pays no heed to a reference Higgs mass and has no direct dependence on the PNGB masses for $N_f = 6$. On the other hand, the stronger UV convergence of the integral expression (Eq. 1) could make single-pole dominance more reliable than for the WSRs. In fact, evaluation of the above expression using our simulation data leads, for $N_f = 2$, to a result within 30% of our direct simulation of S at the smaller M_P^2 values. For $N_f = 6$, the agreement with the direct simulation is at least as good, and, importantly, shows the relative decrease of S per electroweak doublet.

Conclusions We have described a lattice simulation of the masses and decay constants of the lowest-lying vector and axial resonances, and the electroweak S parameter, in an $SU(3)$ gauge theory with $N_f = 2$ and 6 fermions in the fundamental representation. The spectrum becomes more parity doubled and the S parameter per electroweak doublet decreases when N_f is increased from 2 to 6. The final value of S for any $N_f > 2$ will depend logarithmically on the masses of PNGBs, generated by SM and other physics not included here. It will be interesting to study these trends as N_f is increased further, toward N_f^c.

Acknowledgements We thank the Aspen Center for Physics, and the LLNL Multiprogrammatic and Institutional Computing program for time on the BlueGene/L supercomputer. This work was supported by the NNSA and Office of Science of the U.S. Department of Energy, and by the U.S. National Science Foundation.

[1] T. Appelquist, A. Avakian, R. Babich, R. C. Brower, M. Cheng, M. A. Clark, S. D. Cohen, G. T. Fleming, J. Kiskis, E. T. Neil, J. C. Osborn, C. Rebbi, D. Schaich, and P. Vranas, Phys. Rev. Lett. **104**, 071601 (2010), 0910.2224.
[2] T. Appelquist, G. T. Fleming, and E. T. Neil, Phys. Rev. Lett. **100**, 171607 (2008), 0712.0609; Phys. Rev. **D79**, 076010 (2009), 0901.3766.
[3] Z. Fodor, K. Holland, J. Kuti, D. Nogradi, and C. Schroeder (2009), 0907.4562.
[4] K.-i. Nagai, G. Carrillo-Ruiz, G. Koleva, and R. Lewis (2009), 0908.0166.
[5] L. Del Debbio, B. Lucini, A. Patella, C. Pica, and A. Rago, Phys. Rev. **D82**, 014510 (2010), 1004.3206.
[6] A. Hasenfratz, Phys. Rev. **D82**, 014506 (2010), 1004.1004.
[7] T. Appelquist and F. Sannino, Phys. Rev. **D59**, 067702 (1999), hep-ph/9806409.
[8] S. D. H. Hsu, F. Sannino, and J. Schechter, Phys. Lett. **B427**, 300 (1998), hep-th/9801097.
[9] M. Kurachi and R. Shrock, Phys. Rev. **D74**, 056003 (2006), hep-ph/0607231.
[10] M. E. Peskin and T. Takeuchi, Phys. Rev. **D46**, 381 (1992).
[11] C. Allton et al. (RBC-UKQCD), Phys. Rev. **D78**, 114509 (2008), 0804.0473.
[12] P. Boyle, L. Del Debbio, J. Wennekers, and J. Zanotti (RBC-UKQCD), Phys. Rev. **D81**, 014504 (2010), 0909.4931.
[13] E. Shintani et al. (JLQCD), Phys. Rev. Lett. **101**, 242001 (2008), 0806.4222.
[14] C. Amsler et al. (PDG), Phys. Lett. **B667**, 1 (2008).
[15] N. Isgur, C. Morningstar, and C. Reader, Phys. Rev. **D39**, 1357 (1989).
[16] M. A. Shifman, A. I. Vainshtein, and V. I. Zakharov, Nucl. Phys. **B147**, 448 (1979).